arXiv:cond-mat/0511700v1 [cond-mat.other] 29 Nov 2005

Noise Correlations of Hard-core Bosons: Quantum Coherence and Symmetry Breaking

Ana Maria Rey [1,2] *, Indubala I Satija [2,3] † and Charles W Clark[2]
[1]Institute for Theoretical Atomic, Molecular and Optical Physics,
Harvard-Smithsonian Center of Astrophysics, Cambridge, MA, 02138.
[2]National Institute of Standards and Technology, Gaithersburg, MD 20899 and
[3] Dept. of Phys., George Mason U., Fairfax, VA, 22030

(Dated: February 2, 2008)

Noise correlations, such as those observable in the time of flight images of a released cloud, are calculated for hard-core bosonic (HCB) atoms. We find that the standard mapping of HCB systems onto spin-$1/2$ XY models fails in application to computation of noise correlations due to the contribution of *multiply occupied virtual states* in HCB systems. Such states do not exist in spin models. An interesting manifestation of such states is the breaking of particle-hole symmetry in HCB. We use noise correlations to explore quantum coherence of strongly correlated bosons in the fermionized regime with and without external parabolic confinement. Our analysis points to distinctive new experimental signatures of the Mott phase.

In recent years, great experimental progress has been achieved in the coherent control of ultra-cold gases, which has been used to attain laboratory demonstrations of iconic model quantum many-body systems. For example, by loading a Bose-Einstein condensate (BEC) into a tight two-dimensional optical lattice, an array of one-dimensional tubes has been created [1, 2, 3, 4, 5]. Using this setup, recent experiments have been able to successfully enter the Tonks-Girardeau (TG) regime [3, 4] predicted many years ago [6]. Furthermore, by using an additional one-dimensional optical lattice in the direction of the tubes, a one-dimensional Mott insulator (MI) state with unit filling has been realized experimentally [3]. In the TG limit, bosons behave like impenetrable particles - hard-core bosons (HCB) - and their dynamics are equivalent in many respects to those of a system of fermions. In this paper, we calculate four-point correlation functions of HCB and the corresponding spin-$1/2$ and fermion systems.

Experimental access to such correlation functions has recently been achieved [7, 8] by analysis of spatial (noise) correlations in shot-noise-limited images of expanded atomic clouds, following the original suggestion of Altman *et al.* [9]. For example, for the case of bosons in a three-dimensional MI state, these noise correlations have been proven to complement the standard, first-order, characterization of phase coherence that is expressed by the direct image of the density of the expanded gas [8, 9]. Such correlations have also been used to probe pair correlations of fermionic atoms generated by molecular dissociation [7].

In this paper, we develop a theoretical framework to compute noise correlations for HCB systems confined in a one-dimensional lattice. The Hamiltonian of this HCB system is related to that of the spin-$1/2$ XY model, which in turn can be mapped onto the Hamiltonian of a spinless fermion system [10, 11]. These three systems have identical spectra and local observables, but their off-diagonal correlation functions differ. Experimentally relevant two-point correlation functions are identical for HCB and spin-$1/2$ systems, and the general formulation to calculate these correlations was developed by Lieb and Mattis [10, 11], based on Wick's theorem. To our knowledge, explicit formulae to calculate higher order correlations have not been worked out previously, except in certain asymptotic limits [19].

Here we calculate all four-point correlation functions and use them to compute noise correlations. One of the central results of this paper is the discovery of important differences between noise correlation functions of HCB and spin-$1/2$ systems. The root of this difference is the bosonic character of HCB that allows for *multiple occupancy of the virtual states* (MOV) even though the ground state is at most singly occupied. This is in contrast to spin-$1/2$ systems whose Hilbert space excludes multiple occupancy of all states. Here we show that the standard Lieb and Mattis [10, 11] formulation for spin $1/2$ systems can still be utilized for calculating correlations functions in HCB systems provided the operators are written in normal order form by using boson commutation rules, before applying any transformation.

Our study shows that MOV states are responsible for various differences between the HCB and the XY spin-$1/2$ correlations. One particular way to characterize this difference is the particle-hole symmetry: in HCB noise correlations, this symmetry is broken while it is preserved in the corresponding spin systems.

We use the noise correlations to characterize quantum coherence in both homogeneous lattice systems and systems subject to external parabolic confinement, as is often the case in experiments. Previous studies of noise correlations have been carried out in the MI limit [8, 9]; our analysis extends this understanding into the strongly correlated (fermionized) regime. We show that, *independent of the filling factor of the system*, HCB exhibit second order coherence. It is manifested by peaks in the noise shot images which reflect the order induced by the lattice potential. This suggests that second order coherence in noise correlations is a generic attribute of correlated bosonic systems; as was also noted in earlier studies in a different context [9, 12], such coherence does not merely signal reduced number fluctuations. Our detailed study involving all fillings factors highlights distinctions

---

* Electronic address: arey@cfa.harvard.edu
† Electronic address: isatija@physics.gmu.edu

between the Mott regime and the compressible regime. In the MI limit, the intensity of the density-density correlations between any two points separated by a reciprocal lattice vector is constant. In the compressible phase, on the other hand, the corresponding noise correlations depend strongly on the spatial position in the image. Thus a regular pattern in noise correlations could serve as a definite signature of the Mott phase. Additionally, the peaks of noise correlations in the compressible phase are accompanied by satellite dips immersed in a negative background. These dips are suppressed in the insulating phase.

In Section I, we discuss various Hamiltonians related to HCBs and describe noise correlations that can be measured in experiments involving cold atoms in optical lattices. In Section II, we develop the theoretical framework needed to calculate all four point correlation functions relevant for computing noise correlations. In view of the relationships among HCB, XY spin-$1/2$, and spinless fermion models, we develop explicit formulas to calculate noise correlations for all of them. In Section III, we use the formulation of section II to study noise correlations for a spatially homogeneous gas of HCB. We discuss their basic properties and describe in detail how the strengths of the peaks and dips depend upon the filling factors. Our detailed numerical studies suggest that although the peak and dip amplitudes depend upon the size of the system, the peak to dip ratio is size independent. We compare noise correlations for HCB, spin-$1/2$ XY chains, and the corresponding fermionic systems, and show that the spin noise correlations preserve the particle-hole symmetry of the Hamiltonian, but that this symmetry is broken in HCBs. In Section IV, we compute the noise correlations for experimentally relevant parameters and compare results for Mott vs. compressible phases. Section V summarizes our results.

I. INTRODUCTION AND FORMULATION

A. Bose-Hubbard Hamiltonian and Observable

The Bose-Hubbard Hamiltonian describes bosons in optical lattices when the lattice is loaded in such a way that only the lowest vibrational level of each lattice site is occupied and tunneling occurs only between nearest-neighbor sites [13, 20]:

$$\hat{H} = -J \sum_{\langle i,j \rangle} \hat{a}_i^\dagger \hat{a}_j + \frac{U}{2} \sum_j \hat{n}_j(\hat{n}_j - 1) + \sum_j V_j \hat{n}_j \tag{1}$$

Here $\hat{a}_j$ is the bosonic annihilation operator of a particle at site j, $\hat{n}_j = \hat{a}_j^\dagger \hat{a}_j$, and the sum $\langle i,j \rangle$ is over nearest neighbors. The hopping parameter J, and the on-site interaction energy U are functions of the lattice depth. V_j represents any other external potential such as a parabolic confinement or on-site disorder.

In a typical experiment, atoms are released by turning off the external potentials at time $t = 0$. The atomic cloud expands, and is photographed after it enters the ballistic regime. Assuming that the atoms are noninteracting from the time of release, properties of the initial state can be inferred from the spatial images. As explained in detail in Ref. [9, 14], the density distribution after the release, $\langle \hat{n}[x] \rangle = \langle \hat{\psi}(x,t)^\dagger \hat{\psi}(x,t) \rangle$, with $\hat{\psi}(x,t)$ the bosonic field operator, can be written in terms of the first band annihilation and destruction operators at lattice sites as $\sum_{i,j} w^*(x - ia, t) w(x - ja, t) \langle \hat{a}_i^\dagger \hat{a}_j \rangle$ where $w(x,t)$ is the free evolution of a Wannier function centered around the origin and a is the lattice spacing. Assuming the Wannier functions can be described by Gaussians with initial width $\sigma_o/2$, after time of flight t, the spatial density at position x, $\langle \hat{n}[x] \rangle$, can be written as

$$\langle \hat{n}[x] \rangle = w^2(x,t) \sum_{n,m} e^{iP(x,t)a[n-m]} \langle \hat{a}_n^\dagger \hat{a}_m \rangle \propto \langle \hat{n}_Q \rangle, \tag{2}$$

$$\langle \hat{n}_Q \rangle \equiv \frac{1}{L} \sum_{n,m} e^{iQa(n-m)} \langle \hat{a}_n^\dagger \hat{a}_m \rangle, \tag{3}$$

where $w^2(x,t) = \sqrt{\frac{2}{\pi\sigma^2}} e^{-2x^2/\sigma^2}$ and $\sigma = \hbar t/(M\sigma_o)$. The wave-vector $P(x,t) = Mx/(\hbar t)$ defines a correspondence between the position in the expanding image, x, and the lattice wave vector, Q. Here M is the particle mass and L is the number of lattice sites.

Density-density correlations in the expanding cloud, $\mathcal{G}[x,x']$, can also be linked to initial correlations in the lattice. For the evaluation of $\mathcal{G}[x,x']$ it is important to keep in mind that only normal ordered expectation values can be safely replaced by its projection into the lowest band. The second order correlation $\mathcal{G}[x,x']$ is given by [9]:

$$\begin{aligned} &\mathcal{G}[x,x'] = \\ &(w(x)w(x'))^2 \sum_{n,m,l,j} e^{iP(x,t)a[n-m]} e^{iP(x',t)a[l-j]} \langle \hat{a}_n^\dagger \hat{a}_l^\dagger \hat{a}_j \hat{a}_m \rangle \\ &+ w^2(x)\delta(x-x')\langle \hat{n}[x] \rangle - \langle \hat{n}[x] \rangle \langle \hat{n}[x'] \rangle \end{aligned} \tag{4}$$

where $\delta(x-x') = L\delta_{x,x'}$ is a delta function which arises from normal ordering in the continuum. Eq. (4) can be mapped to quasi-momentum correlations in the lattice, $\mathcal{G}[x,x'] \rightarrow \Delta(Q,Q')$, as:

$$\begin{aligned}\Delta(Q,Q') \;&\equiv\; \langle \hat{n}_Q \hat{n}_{Q'}\rangle - \langle \hat{n}_Q\rangle\langle \hat{n}_{Q'}\rangle \\ &-\; \langle \hat{n}_Q\rangle(\delta_{Q,Q'+nK} - \delta_{Q,Q'}),\end{aligned} \tag{5}$$

where $K = 2\pi/a$ is the reciprocal lattice vector and n is an integer. The first term in the second line of Eq. (5) arises due to the bosonic commutation relations of the operators and the identity $1/L\sum_{l=1}^{L} e^{i2\pi mnl/L} = \delta_{m,nL}$. The quantity $\Delta(Q,Q') \equiv \Delta_{qq'}$, that corresponds to density-density correlations in the expanding cloud of atoms, will be referred to as the *noise correlations*. The integer q characterizes the discrete values of the quasimomentum $Q = \frac{2\pi}{La}q$ and this convention is going to be used hereafter.

B. Hard Core Bosons (HCB)

In the strongly correlated regime, Eq. (1) can be replaced by the HCB Hamiltonian [20],

$$\hat{H}^{(HCB)} = -J\sum_j(\hat{b}_j^\dagger\hat{b}_{j+1} + \hat{b}_{j+1}^\dagger\hat{b}_j) + \sum_j V_j\hat{n}_j \tag{6}$$

Here $\hat{b}_j$ is the annihilation operator at the lattice site j which satisfies $[\hat{b}_{i\neq j}, \hat{b}_j^\dagger] = 0$, and the on-site conditions $\hat{b}_j^2 = \hat{b}_j^{\dagger 2} = 0$, which suppress multiple occupancy of lattice sites. The same relations are fulfilled by spin-1/2 raising and lowering operators, $\hat{\sigma}_j^{\pm}$, and this is the reason why the HCB Hamiltonian is mapped to the spin $1/2$ -XY Hamiltonian,

$$\hat{H}^{(\sigma)} = -2J\sum_j(\sigma_j^x\sigma_{j+1}^x + \sigma_j^y\sigma_{j+1}^y) + V_j\sum_j\frac{\sigma_j^z+1}{2} \tag{7}$$

Here σ_l are Pauli matrices that satisfy anti-commutation relation at same sites. The parameter J describes the exchange interaction between the XY-spins. A fully polarized state with all spins up corresponds to the Mott insulator state. We would like to emphasize that the mapping between the HCB and the spin Hamiltonian is a partial mapping as the two differ in the onsite commutation relation.

For spin-1/2 systems, correlation functions are in general calculated by using the Jordan-Wigner transformation (JWT) [10, 20] which maps spin operators into fermionic operators $\hat{\sigma}_j^+ = \hat{c}_j^\dagger \exp\left[-\pi i\sum_{n=1}^{j-1}\hat{c}_n^\dagger\hat{c}_n\right]$. Here $\hat{c}_j$ are fermion operators that obey anticommutation relations. This transformation maps the spin Hamiltonian into a non-interacting fermionic Hamiltonian,

$$H^{(F)} = -J\sum_j(\hat{c}_j^\dagger\hat{c}_{j+1} + \hat{c}_{j+1}^\dagger\hat{c}_j) + \sum_j V_j\hat{n}_j. \tag{8}$$

Two-point HCB correlations have been calculated by invoking the HCB→ spin-$1/2$ → fermion correspondence [17]. As mentioned above, in contrast to the spin operators which obey fermionic commutation relations at the same site, HCB operators at equal sites obey bosonic commutation relations. Correlation functions such as $\langle\phi|\hat{O}\hat{O}^\dagger|\phi\rangle$ (where we have suppressed the lattice index for convenience) are zero if $\hat{O}$ are spin lowering operators and non-zero if $\hat{O}$ are HCB field operators. The non-vanishing of these correlations can be traced to the fact that the HCB may have virtual states that have multiple occupancy: Recall that the HCB describes the $U\rightarrow\infty$ limit of the Bose-Hubbard Hamiltonian, and therefore, the limiting value of the Bose-Hubbard correlation functions must correspond to those of HCB. In general for bosons one can write $|\phi\rangle = A|0\rangle + B|1\rangle + \epsilon|2\rangle + \ldots$ where $\epsilon \sim 1/U$ and A, B are constants. Therefore, $\langle\phi|\hat{a}\hat{a}^\dagger|\phi\rangle = A^2 + 2B^2 + 3\epsilon^2 + \ldots$. Taking the $U\rightarrow\infty$ limit one gets $\langle\phi|\hat{a}\hat{a}^\dagger|\phi\rangle \rightarrow A^2 + 2B^2 > 0$. On the other hand this correlation is always zero for the spin systems.

The differences in the on-site commutation rules for bosons and spins have no effect on the calculations of local observables such as the density and the momentum distribution. However, correlation functions that involve a pair of operators $\hat{b}_j\hat{b}_j^\dagger$, are affected by MOV states. In such cases, a direct application of the JWT is not correct. A simple recipe to take into account the MOV problem is to replace $\hat{b}_j\hat{b}_j^\dagger$ by $1 + \hat{b}_j^\dagger\hat{b}_j$ before applying the JWT. We will refer to this recipe as the MOV rule. The validity of the MOV rule was checked by comparing various correlation functions obtained using the above recipe with those obtained by diagonalizing a full Bose-Hubbard Hamiltonian with a large U value (see below).

II. FOUR-POINT CORRELATIONS

We now describe our calculations of four-point correlations. In view of the rather complex nature of the calculations, we will omit various technical details but focus on describing the final formulas and notations so that our results can be used for related future work. In addition to HCB, we will also discuss the related fermion and spin systems.

For ideal fermions, four point correlation functions can be calculated using Wick's theorem directly. For example, the four-point correlations relevant for noise correlation are given by:

$$\langle \hat{c}_n^\dagger \hat{c}_m \hat{c}_l^\dagger \hat{c}_j \rangle = -\delta_{lm} g_{nj} + g_{lj} g_{nm} - g_{lm} g_{nj}, \tag{9}$$

where g_{lm} are free-fermionic propagators:

$$g_{lm} = \sum_{s=0}^{N-1} \psi_l^{*(s)} \psi_m^{(s)}, \tag{10}$$

with N being the total number of atoms and $\psi_l^{(s)}$ the s^{th} eigenfunctions of the single-particle Hamiltonian $-J(\psi_{l+1}^{(s)} + \psi_{l-1}^{(s)}) + V_l \psi_l^{(s)} = E^{(s)} \psi_l^{(s)}$.

For HCB and spin systems, the calculation of four-point functions is more complex. Specifically, our calculations involve the following steps. (i) rearrange the operators so that the site index is ordered (this is only relevant for the case when three or more site indices are different); (ii) write operators in normal order form using bosonic rules to take into account the MOV; (iii) use the JWT accordingly to the prescription of Lieb and Mattis; (iv) use Wick's theorem to write higher order correlations in terms of two-point correlations.

To present our results we denote the creation and the annihilation operators by $\hat{b^{\alpha}}$, where $\alpha = +1(-1)$ for annihilation (creation) operators, respectively, and label the "site ordered" four-point correlation function by $\chi_{abcd}^{\alpha\beta\gamma\delta}$

$$\langle \hat{b}_n^\dagger \hat{b}_m \hat{b}_l^\dagger \hat{b}_j \rangle \mapsto \langle \hat{b}_a^{(\alpha)} \hat{b}_b^{(\beta)} \hat{b}_c^{(\gamma)} \hat{b}_d^{(\delta)} \rangle \equiv \chi_{abcd}^{\alpha\beta\gamma\delta}, \tag{11}$$

In this equation it is implicit that $a \leq b \leq c \leq d$. This order is implied in all the expressions that follow. We define $G_{ij} \equiv 2g_{ij} - \delta_{i,j}$ and $B_{ij} \equiv \langle \hat{b}_i^{(\dagger)} \hat{b}_j \rangle$. The latter can be calculated in terms of G_{ij} [11]. We introduce four matrices $\mathbf{M}, \mathbf{S}, \mathbf{X}$ and $\mathbf{Y}$ in terms of which our results for the correlation functions can be written as

$$\chi_{abbd}^{\alpha\beta\gamma\delta} = \frac{\beta\gamma - 1}{2} \left[\frac{(-1)^{s\eta_\beta}}{4} |\mathbf{M}(a,b,d)| - \left(\frac{1}{2} + (1-s)\delta_{\beta,-1} \right) B_{ad} \right], \tag{12}$$

$$\chi_{aacd}^{\alpha\beta\gamma\delta} = \frac{1 - \alpha\beta}{2} \left[\frac{(-1)^{s\eta_\alpha}}{4} |\mathbf{S}(a,c,d)| + \left(\frac{1}{2} + (1-s)\delta_{\alpha,-1} \right) B_{cd} \right], \tag{13}$$

$$\chi_{abcc}^{\alpha\beta\gamma\delta} = \frac{1 - \gamma\delta}{2} \left[\frac{1}{4} (-1)^{s\eta_\gamma} |\mathbf{S}(c,a,b)| + \left(\frac{1}{2} + (1-s)\delta_{\gamma,-1} \right) B_{ab} \right], \tag{14}$$

$$\chi_{abcd}^{\alpha\beta\gamma\delta} = (-1)^{b+d-c-a} \left[\frac{2 - \gamma\delta - \alpha\beta}{16} |\mathbf{X}(a,b,c,d)| + \frac{\beta}{4} (\delta_{\gamma,-1} - \delta_{\alpha,-1}) |\mathbf{Y}(a,b,c,d)| \right]. \tag{15}$$

$$\mathbf{M} = \begin{pmatrix} G_{aa+1} & G_{ab-1} & G_{ab+1} & .. & G_{ac} \\ \vdots & & & & \vdots \\ G_{b-1a+1} & G_{b-1b-1} & G_{b-1b+1} & .. & G_{b-1c} \\ G_{b+1a+1} & G_{b+1b-1} & G_{b+1b+1} & .. & G_{b+1c} \\ \vdots & & & & \vdots \\ G_{c-1a+1} & G_{c-1b-1} & G_{c-1b+1} & .. & G_{c-1c} \end{pmatrix}, \tag{16}$$

$$\mathbf{X} = \begin{pmatrix} G_{ba} & .. & G_{bb-1} & G_{bc+1} & .. & G_{bd-1} & G_{bc} \\ G_{a+1a} & .. & G_{a+1b-1} & G_{a+1c+1} & .. & G_{a+1d-1} & G_{a+1c} \\ \vdots & & & & & \vdots & \\ G_{b-1a} & .. & G_{b-1b-1} & G_{b-1c+1} & .. & G_{b-1d-1} & G_{b-1c} \\ G_{c+1a} & .. & G_{c+1b-1} & G_{c+1c+1} & .. & G_{c+1d-1} & G_{c+1c} \\ \vdots & & & & & \vdots & \\ G_{da} & .. & G_{db-1} & G_{dc+1} & .. & G_{dd-1} & G_{dc} \end{pmatrix}, \tag{17}$$

$$\mathbf{S} = \begin{pmatrix} G_{aa} & G_{ab+1} & .. & G_{ac} \\ G_{ba} & G_{bb+1} & .. & G_{bc} \\ \vdots & & & \vdots \\ G_{c-1a} & G_{c-1b+1} & .. & G_{c-1c} \end{pmatrix}, \tag{18}$$

$$\mathbf{Y} = \begin{pmatrix} G_{a+1a} & G_{a+1b} & G_{a+1a+1} & .. & G_{a+1b-1} & G_{a+1c+1} & .. & G_{a+1d-1} \\ \vdots & & & & & & & \vdots \\ G_{b-1a} & G_{b-1b} & G_{b-1a+1} & .. & G_{b-1b-1} & G_{b-1c+1} & .. & G_{b-1d-1} \\ G_{c+1a} & G_{c+1b} & G_{c+1a+1} & .. & G_{c+1b-1} & G_{c+1c+1} & .. & G_{c+1d-1} \\ \vdots & & & & & & & \vdots \\ G_{d-1a} & G_{d-1b} & G_{d-1a+1} & .. & G_{d-1b-1} & G_{d-1c+1} & .. & G_{d-1d-1} \\ G_{ca} & G_{cb} & G_{ca+1} & .. & G_{cb-1} & G_{cc+1} & .. & G_{cd-1} \\ G_{da} & G_{db} & G_{da+1} & .. & G_{db-1} & G_{dc+1} & .. & G_{dd-1} \end{pmatrix}. \tag{19}$$

Here s is equal to 0 for HCB and 1 for spins and $\eta_\beta = \delta_{\beta,-1}$. In the matrices dots indicate continuous variation of the indices. In the absence of dots, the indices are explicitly written and they may not change continuously.

When three, four or two pairs of indices are equal the calculation of the four-point functions is simple and no determinant is actually required. The non-vanishing correlation functions of this type are given by:

$$\langle \hat{b}_n^\dagger \hat{b}_n \hat{b}_n^\dagger \hat{b}_n \rangle = g_{nn}, \tag{20}$$

$$\langle \hat{b}_n^\dagger \hat{b}_n \hat{b}_m^\dagger \hat{b}_m \rangle = g_{nn} g_{mm} - g_{nm}^2, \tag{21}$$

$$\langle \hat{b}_n^\dagger \hat{b}_m \hat{b}_m^\dagger \hat{b}_n \rangle = (-1)^s (g_{nn} g_{mm} - g_{nm}^2) + g_{nn}, \tag{22}$$

$$\langle \hat{b}_n^\dagger \hat{b}_n \hat{b}_n^\dagger \hat{b}_m \rangle = \langle \hat{b}_m^\dagger \hat{b}_n \hat{b}_n^\dagger \hat{b}_n \rangle = B_{nm}. \tag{23}$$

with $n \neq m$ and $B_{ij} \equiv \langle \hat{b}_i^{(\dagger)} \hat{b}_j \rangle$. The latter can be calculated in terms of G_{ij} [11].

III. NOISE CORRELATIONS FOR HOMOGENEOUS SYSTEMS

We now analyze various characteristics of the noise correlations that are calculated using the formulation discussed above. We consider particles in a periodic lattice in the absence of any external potential ($V_i = 0$). Here we compare and contrast HCB, XY spin-$1/2$ and the corresponding fermion system. This comparison illustrates the importance of MOV and the quantum statistics of the particles in noise correlations. Our study includes all filling factors ν, $0 \leq \nu \leq 1$. Here $\nu = N/L$ where L is the number of lattice sites and N is the total number of particles. We thus study the Mott regime ($\nu = 1$) as well as the non-Mott regime with $1 < \nu < 1$.

For the HCB and the spin systems the Töplitz-like determinants involved in the evaluation of noise correlations make the calculations complicated. The only simple case that can be studied analytically is when the system is a MI ($\nu = 1$). In this case, $g_{ji} = \delta_{i,j}$ and the determinants involved in the calculation become trivial. The noise correlations are given by

$$\Delta^{HCB}(Q_1, Q_2)|_{\nu=1} = \delta_{Q_1,Q_2} + \left(\delta_{Q_1,Q_2+jK} - \frac{2}{L} \right), \tag{24}$$

where j is an integer. Eq. (24) shows the characteristic bosonic peaks at every reciprocal lattice vectors, which reflect the order induced by the periodicity of the lattice. The peaks in HCB correlations reflect the bunching of the bosons due to Bose-Einstein statistics. It should be noted that the noise correlations at $Q_1 = Q_2$ (autocorrelations) are different from those at $Q_1 = Q_2 + Kj$, ($j \neq 0$). For a unit filled MI in particular, the former is two times larger than the latter ,$\Delta(Q_1, Q_1) = 2\Delta(Q_1, Q_1 + Kj)$.

For spins, $\nu = 1$ corresponds to a fully polarized system. In this case, the local correlations dominate and the spins behave like fermions. The fermion correlations are given by

$$\Delta^F(Q_1, Q_2) = -n_{Q_1}^2 \delta_{Q_1 - Q_2, jK} \qquad j \neq 0, \tag{25}$$

where $n_{Q_1} = 1$ for $[Q_1]_K < Q_F$ and zero otherwise. Here $[]_K$ means modulo reciprocal lattice vectors, j is an integer different from zero and Q_F is the Fermi wave-vector $Q_F = \frac{2\pi \| \nu/2 \|}{a}$(where $\| x \|$ denotes the integer part). The fermionic noise interference pattern shows negative interference dips at every reciprocal lattice vector (except at $Q_1 = Q_2$ where $\Delta(Q_1, Q_1) = 0$) signaling the underlying anti-bunching due to Fermi-Dirac statistics.

From Eqs. (24) and (25) one arrives at the conclusion that in the Mott regime ($\nu = 1$), HCB noise correlations with central peak height equal to 2 differ from the corresponding spin correlations which show no central peak. Thus this simple limit brings out the importance of MOV in HCB.

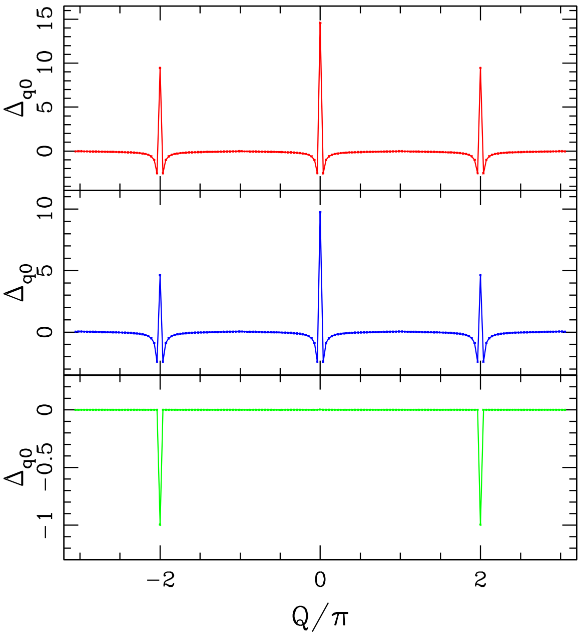

FIG. 1: Noise correlations at $Q_2 = 0$ for different values of $Q = 2\pi q/(La)$ (In the plot the x-axis is in units of $1/a$). The upper, middle and lower panels respectively correspond to HCB, spins and fermions (note the different scale used in the bottom panel). We use $L = 55$ and $N = 27$.

For non-integer filling factors $0 < \nu < 1$, there is no simple analytic expression for the noise correlations. Therefore, all four point functions and the noise correlations are computed numerically. Our detailed investigation included lattices of various sizes and we studied both fixed end as well as periodic boundary conditions. Fig. 1 illustrates the quantum coherence of HCB, spin and fermions as characterized by Δ_{q0}. Our calculations show that for HCB as well as for spin systems noise correlations exhibit characteristic peaks at every reciprocal lattice vector for all filling factors. These peaks reflect the underlying order induced by the periodic lattice. The heights of the peak vary with the filling factor (see Fig. 2). The peaks are a manifestation of the boson nature of the atoms and are induced by interactions as they disappear in the non-interacting regime where all of the atoms are Bose-condensed. For fractional values of ν, the peaks are accompanied by a small satellite dip at $Q = 2\pi/(La) + jK$ immersed in a negative background. In other words, the dips occur only in the compressible phase. These dips are present only for non-integer filling factor and are a manifestation of the quasi-long range coherence of the system.

It turns out that Bogoliubov theory [15] is helpful in gaining insight into the the dips and the negative background in the HCB noise correlations. The theory describes the weakly interacting regime and in principle can not be used to quantitatively describe the HCB gas. However, some aspects of the theory survive in HCB limit and suggest a possible mechanism for the dips and the negative background that characterize the compressible regime. The Bogoliubov approximation predicts the negative background $\Delta(0, Q) < 0$ and the satellite dip at low quasi-momenta (phonon regime). In the thermodynamic limit $\Delta(0, Q)$ diverges as $-\frac{\nu U}{4JQ^2}$. For finite lattices the height of the satellite dip does not diverge but scales like $-\frac{\nu U}{4J}\frac{L^2}{4\pi^2}$. Moreover in the Bogoliubov approximation the central peak scales like $\frac{\nu U}{4J}\frac{L}{2\pi}\cot[\pi/L]$ so the peak to dip ratio remains finite (see also [16]). As we discuss below, the insensitivity of this ratio to the lattice size is also seen in HCB case.

The negative background, $\Delta(0, Q) < 0$, and the satellite dip at low quasi-momenta can also be qualitatively understood as follows: $\Delta(0, Q)$ can be written as $\Delta(0, Q) = \langle e|e\rangle - N_0 n_Q$ where N_0 is the number of condensate atoms, n_Q is the number of atoms with quasi-momenta $\hbar Q$ (the population of which comprises the quantum depletion) and $\langle e|e\rangle$ is the amplitude of the state $|e\rangle = |\hat{a}_Q \hat{a_0}|g\rangle$, with $|g\rangle$ the many-body ground state. $|e\rangle$ represents the process of removing a particle from the condensate and one from the state with quasi-momentum $\hbar Q$. In the absence of interactions all of the atoms are Bose condensed, correlations can be neglected and $\langle e|e\rangle = N_0 n_Q = 0$. On the other hand, interactions dramatically change the behavior of the Bose gas. Collisions between zero-quasimomentum atoms admix into the condensate pairs of atoms at quasimomenta $\pm\hbar Q$. As a result pair excitations in the condensate become correlated so as to minimize the total energy of the system giving rise to the negative sign in the noise correlations. For high quasi-momenta the interference plays a minor role but in the phonon regime n_{-Q} diverges and the anti-correlations are maximal.

As mentioned above for HCB bosons Bogoliubov theory is not qualitatively valid but it still gives a useful physical picture as the HCB ground state also exhibits off-diagonal quasi-long-range order that manifests in the power law decay of the density matrix and the macroscopic occupation of the zero quasi-momentum state (quasi-condensate) which scales like $\sqrt{N}$ [17] (see Fig. 5).

In Fig. 2 we study the dependence of the peak and dip height with the filling factor for HCB and the correspondent spin system. As illustrated there the heights (Δ_{00}) and the dips ($|\Delta_{10}|$) of the peaks increase with the filling factor up to a maximum value and then begin to decrease. At $\nu = 1$, for HCB, the height approaches 2 while the dip vanishes ($\Delta(Q,0) \to -2/L$). However, for the spin model, the corresponding value is 0 for both peak and dip.

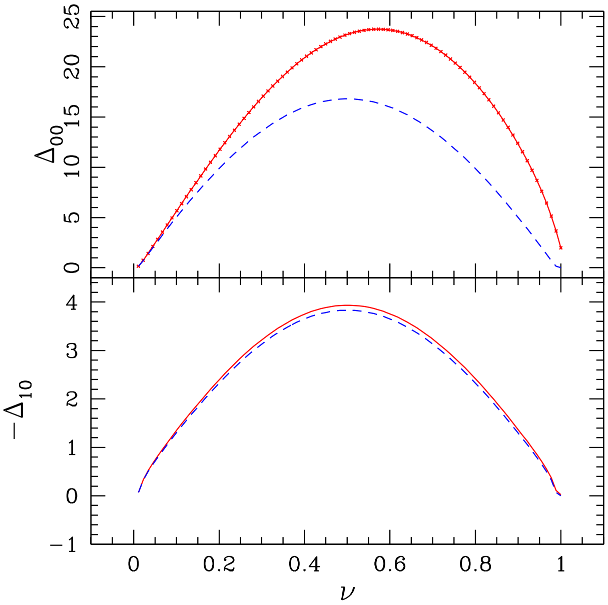

FIG. 2: The figure shows the central peak at occurs at $q = q' = 0$(top) and the the corresponding satellite dip intensity at $q = 1$ and $q' = 0$ as we vary the filling factor. Red and blue respectively correspond to HCB and spin systems. Here $L = 89$ and we use free boundary conditions.

The central peak attains its maximum value at $\nu \approx 0.6$ and the curve describing the variation of its height with the filling factor lacks reflection symmetry about $\nu = 1/2$. These results were confirmed for various lattice sizes as well as for periodic boundary conditions. The asymmetric behavior implies that the noise correlations for HCB do not preserve particle hole symmetry. In contrast, the satellite dip appears to preserve it. The asymmetry in HCB correlations has its roots in the MOV states as the spin correlations (which do not have MOV) preserves the particle-hole symmetry. In fact, the spin Hamiltonian, Eq. (7) with the additional constraints $[\hat{\sigma}^-_{i\neq j}, \hat{\sigma}^+_j] = 0$, and $[\hat{\sigma}^-_i, \hat{\sigma}^+_i]_+ = 1$, is particle-hole symmetric under the transformation $\hat{\sigma}^-_i = \hat{h}^\dagger_i$, $\hat{\sigma}^+_i = \hat{h}_i$. The operators $\hat{h}^\dagger_i$ and $\hat{h}_i$ are the creation and annihilation operator for holes. On the other hand, if $[\hat{\sigma}^-_i, \hat{\sigma}^+_i]_+ = 1$ is replaced by $[\hat{b}_i, \hat{b}^\dagger_i] = 1$, as is the case for HCB, the particle-hole symmetry is no longer preserved under this transformation (which in terms of HCB operators reads as $\hat{b}_i = \hat{h}^\dagger_i$, $\hat{b}^\dagger_i = \hat{h}_i$).

It is important to mention that, in general, different observables do not have to preserve the symmetries of the Hamiltonian. For example, the momentum distribution for spins has an explicit dependence on the density and is not completely symmetric around $\nu = 1/2$ [17]. Nevertheless as shown in Fig. 2, noise-correlations do preserve the particle hole-symmetry of the Hamiltonian.

Our detailed numerics shows that the heights of the peaks and the dips depend upon the lattice size and are expected to diverge in the thermodynamic limit. However, our simulations also suggest that the ratio of height to dip is size independent (behavior also observed in the Bogoliubov calculations) for various filling factors. In particular for HCB the ratio near the maxima of the central peak is found to approach 2π (See Fig. 3). The scale invariance of this ratio makes it a more desirable physical quantity that can be compared in different experiments.

The striking differences between the spins and the HCB noise correlations not only highlight the importance of including MOV states but also explicitly show that a direct mapping between the two systems is not valid for all observables. We checked the validity of MOV rule by calculating noise correlations using a direct diagonalization of the Bose-Hubbard Hamiltonian for small size systems. Fig. 4 illustrates the variation of height of the central peak and the dip as a function of the interaction U. As U increases noise correlations reach the asymptotic value that was found to be in excellent agreement with the value calculated from the HCB model including MOV states. We also calculate the noise correlations for the spin model, to emphasize the fact that MOV corrections can be significant. Even for a small size system, Fig.4 clearly shows broken symmetry for HCB while the symmetry is preserved for the spin system. In Fig. 4 the central peak is found to be associated with a dip for all values of U in consistency with the Bogoliubov calculations.

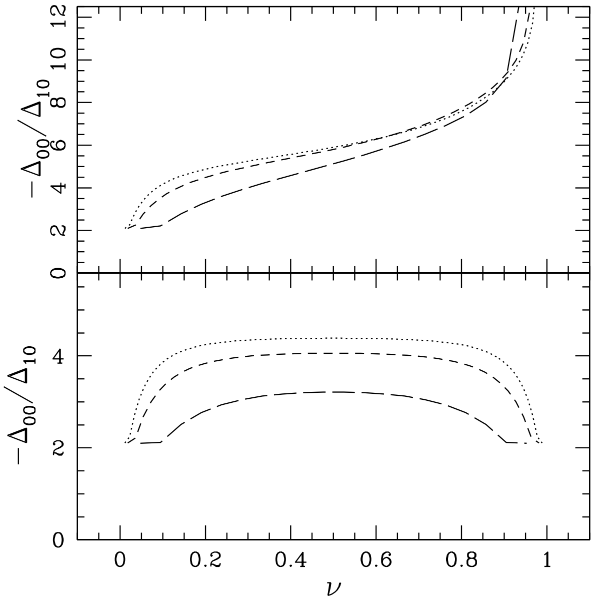

FIG. 3: The upper and the lower panels respectively show the ratio of height to dip for the HCB and spin systems. The three curves in each panel respectively correspond to $L = 89$ (dotted), $L = 55$ (short dashed), $L = 21$ (long dashed) lines.

IV. MOTT VS NON-MOTT PHASE IN A PARABOLICALLY CONFINED CASE

In this section we study noise correlations for the experimentally relevant case when there is an additional parabolic confinement $V_j = \Omega j^2$. The advantage of having the parabolic confinement is that in this case it is always possible to realize a unit MI at the trap center for any number of particles with an appropriate choice of the trapping potentials [17, 18]. In the homogeneous case on the contrary only for the integer filled case is a MI possible. In our analysis, the chosen parameters correspond to typical experimental set-ups such as the ones reported in Ref. [3]. We present our results for two different values of Ω/J, 0.008 and 0.17.

The density profiles (Fig. 5 top panel) show that for the case $\Omega/J = 0.17$ the ground state of the system corresponds to a MI with all the central N sites singly occupied. For $\Omega/J = 0.008$, on the other hand all, the sites have filling factor less than unity. The formation of a MI state with reduced number fluctuations and the localization of the atoms at individual lattice sites are signaled by the momentum distribution (Fig.5 bottom panel), which shows a flat profile for $\Omega/J = 0.17$. On the other hand, the non-vanishing off diagonal coherence and large number fluctuations in the $\Omega/J = 0.008$ case are reflected by the sharp peak in the momentum distribution at $Q = 0$.

In Fig.6 we plot $\Delta(Q_1, Q_2)$ for the Mott and non-Mott systems as a function of Q_1 and Q_2. Noise correlations show interference peaks when $Q_1 = Q_2 + nK$. The existence of these peaks in MI as well as in non-Mott phase implies that the presence of peaks is not a signature of the insulating phase. Our numerical calculations show that, nevertheless, information about the insulator or superfluid character of the system can be extracted from noise-interferometry as only when the system is a MI, the noise-correlations exhibit a regular pattern, i.e. $\Delta(Q_1, Q_2) \approx \Delta(Q_1 - Q_2)$ (small differences seen in Fig. 6 are due to the finite trap). In contrast, when tunneling is allowed and non-local correlations are established, they cause a decay in the intensity of the peaks as one moves away from $[Q_1]_K = [Q_2]_K = 0$. This decay is similar to the one observed in the momentum distribution away from $Q = 0$ and reflects the non-vanishing off-diagonal coherence of the system.

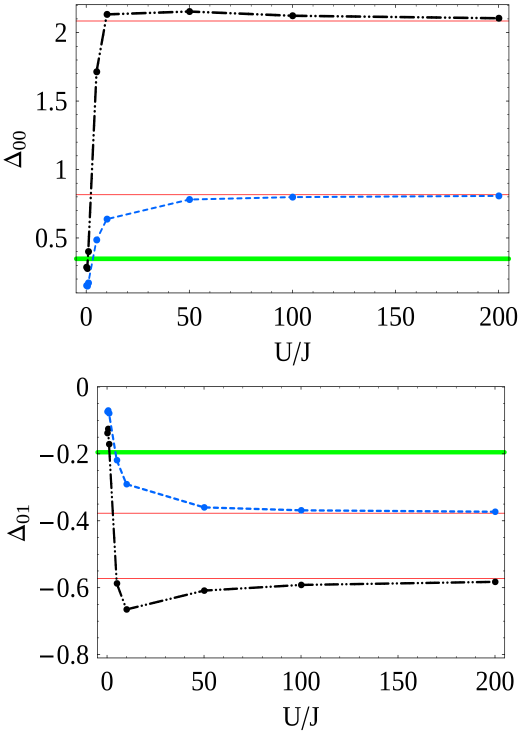

FIG. 4: The figure shows the peak (upper) and the dip(lower) intensities for $L = 6$ and N equal to 2(dashed blue line) and 4 (dotted-dashed black) as the interaction U varies. The solid horizontal red lines show the corresponding result for HCB obtained using the theoretical formulation described in section I. The green(thick) line shows the result without MOV contribution and hence describes the noise correlations for the spin-$1/2$ XY chain. In this case, $\nu = 1/3$ and $2/3$ results coincide reflecting particle-hole symmetry.

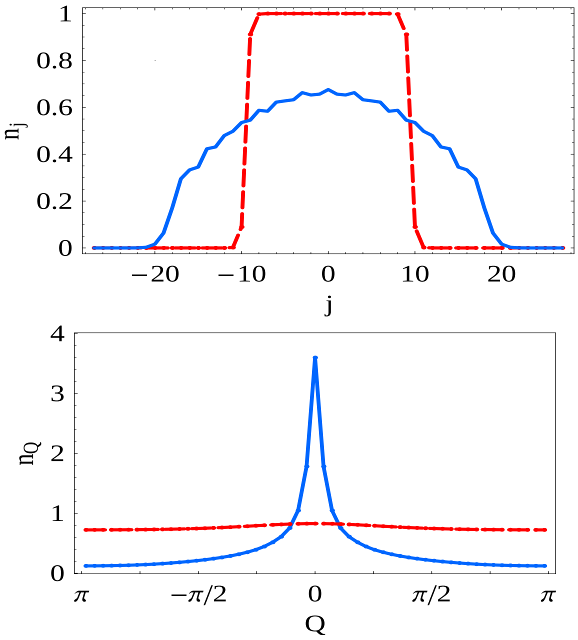

FIG. 5: Top: Density, Bottom: momentum distribution (Q is in units of $1/a$) for different trapping potentials: 0.008(blue solid line), and 0.17 (red dashed-line)). Here $N = 19$ and $L = 55$. The correlation functions are renormalized by a scaling factor N/Z where Z are the number of sites with non-zero density.

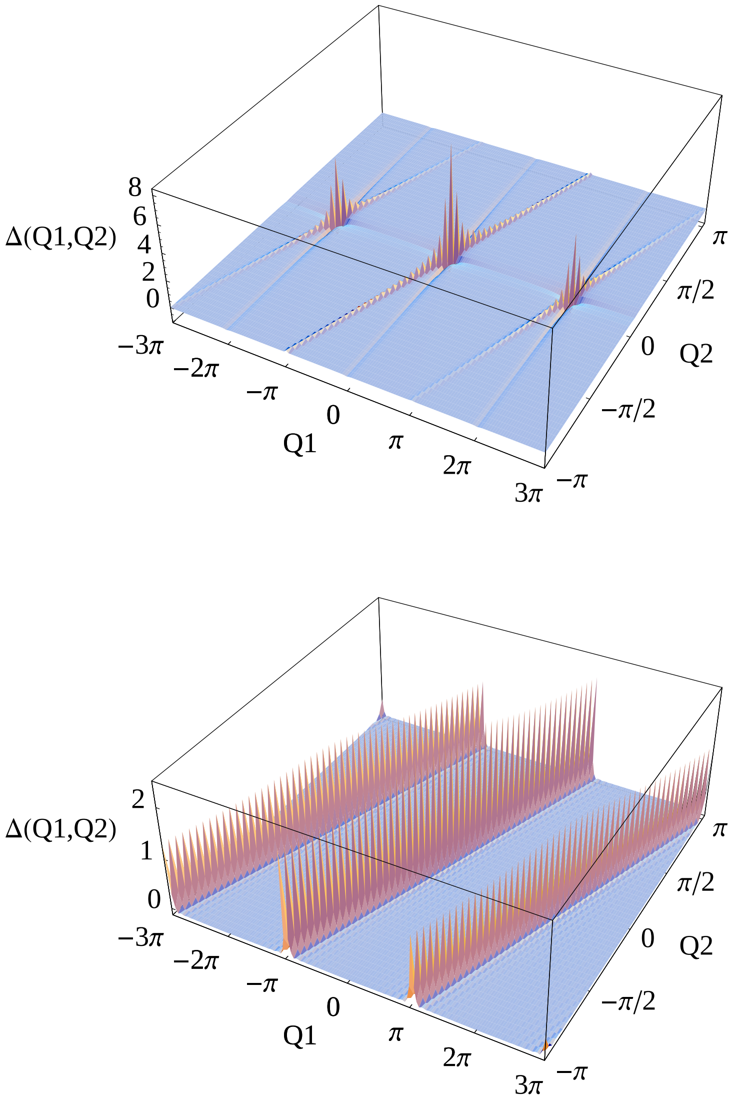

FIG. 6: Noise correlations as a function of Q_1 and Q_2 for the same parameters used in Fig.4. Q_1 and Q_2 are in units of $1/a$. The upper and lower correspond to $\Omega/J = 0.008$(Non MI) and 0.17(MI) respectively. The correlation functions are renormalized by a scaling factor N/Z where Z are the number of sites with non-zero density.

Furthermore, Fig. 6 shows that the satellite dips observed in partially filled translationally invariant systems are still present in the inhomogeneous case. When $\Omega/J = 0.008$ they are located at $[Q_1]_K = 2\pi/(La)$ $[Q_2]_K = 0$ and disappear in the MI phase.

All of these results suggest that noise interferometry provides valuable complementary information about the phase coherence of the system and thus can be a suitable experimental tool for characterizing the MI phase. Experimental techniques capable of thoroughly characterizing the MI phase are crucial for the neutral atom based quantum information proposals.

V. SUMMARY

In this paper, we have derived explicit formulae to calculate four-point functions in HCB, spin-$1/2$ and fermionic systems in the presence of an external potential. Our results are valid for all filling factors and hence include the Mott as well as the non-Mott regimes. Our work generalizes the Lieb and Mattis formulation for two point correlations to four-point correlations and is therefore an asset for all future studies of higher order correlations in HCB as well as in spin-$1/2$ systems.

One of the key results of our studies is the fact that although multiply occupied states are suppressed in the ground state of strongly correlated bosons, MOV states have to be included for a proper calculation of correlations. These states lead to differences between HCB and spin-$1/2$ XY chains which have important manifestations such as the breaking of particle-hole symmetry in the HCB systems. Recently, there have been various proposals to use bosonic atoms in optical lattices as quantum simulators of spins models [21]. Our study points out that such mappings have to be done very carefully as MOV states can certainly change the spin character of certain observables.

We also showed that the noise correlation pattern is a sensitive probe to characterize the MI phase as: i) only in the MI phase is the noise-pattern completely regular, ii) there are additional satellite dips accompanying the Bragg interference peaks in the absence of a MI. These findings might have some impact in current efforts to implement a quantum computer using optical lattices as most of proposals require a well characterized MI state to initialize the quantum register [18].

We would like to emphasize that we have studied experimentally measurable shot noise correlations for strongly correlated bosons in the TG regime. Discussions related to the corresponding spin system is included to highlight the importance of multiple occupancy of virtual states in HCB, as the correlations in the spin systems describe correlations of HCB without MOV. In other words, results for spins are not presented in the context of any experiments in these systems. However, our general expressions for four-point correlations for spins will potentially be very useful for various studies of higher order correlations in spin systems such as XY and Ising chains with or without disorder.

Acknowledgments

We are grateful to Trey Porto for various suggestions and comments. We would like to thank L. Mathey *et. al* [16] for sharing their results (under preparation) of a related study of noise correlations using bosonization techniques where a characteristic peak, followed by a satellite dip (similar to those shown in Fig.1) are found. This work is supported in part by the Advanced Research and Development Activity (ARDA) contract and the U.S. National Science Foundation through a grant PHY-0100767. A.M.R. acknowledges additional support by a grant from the Institute of Theoretical, Atomic, Molecular and Optical Physics at Harvard University and Smithsonian Astrophysical observatory.

[1] Laburthe Tolra B *et al* 2004 *Phys. Rev. Lett.* **92** 190401 .
[2] Moritz H, Stöferle T, Köhl M and Esslinger T 2003 *Phys. Rev. Lett.* **91** 250402.
[3] Paredes B *et al* 2004 *Nature* ***429*** *277.*
[4] Kinoshita T, Wenger T and Weiss D S 2004 Science ***305*** *1125.*
[5] Fertig C D et al 2005 Phys. Rev. Lett. ***94*** *120403.*
[6] Girardeau M 1960 J. Math. Phys. ***1*** *516 .*
[7] Greiner M et al 2005 Phys. Rev. Lett. ***94*** *110401.*
[8] Foelling S et al 2005 Nature ***434*** *481.*
[9] Altman E 2004 et al, Phys. Rev. A ***70*** *013603.*
[10] Lieb E H and Liniger W 1963 Phys. Rev. ***130*** *1605 .*
[11] Lieb E , Schultz T and Mattis D 1961 Ann. Phys. **16** *407.*
[12] Mathey L, Altman E and Vishwanath A 2005 cond-mat /0507108 .
*[13] Jaksch D et al 1998 Phys. Rev. Lett.****81*** *3108.*
[14] Roth R and Burnett K 2003 Phys. Rev. A ***67****031602.*
[15] Bogoliubov N N 1947 J. Phys **11***, 23.*
[16] Similar results using bosonization techniques for 1D systems have been found by Mathey L, Altman E and Vishwanath A . In preparation.
[17] Rigol M and Muramatsu M 2005 Phys. Rev. A ***72*** *013604.*
[18] Pupillo G, Rey AM, Brennen G B , Williams C J , and Clark C W 2004 J. Mod. Opt. ***51*** *2395; Brennen G B , Pupillo G, Rey A M, Clark C W, and Williams CJ 2005 J. Phys. B* **38** *1687.*
[19] Korepin V E , Bogoliubov N M , and Izergin A G 1993 Quantum Inverse Scattering Methods and Correlation Functions, (Cambridge University Press).
[20] Sachdev S 1999 Quantum Phase Transitions (Cambridge University Press).
[21] Duan L M , Demler E and Lukin M D 2003 Phys Rev Lett. **91** *090402.*